J. COMBIN. MATH. COMBIN. COMPUT. 126 (2025) 247–261

Journal of Combinatorial Mathematics
and Combinatorial Computing
www.combinatorialpress.com/jcmcc

Perfect truncated-metric codes in lattice graphs and superlattice graphs

I. J. Dejter[1,✉], L. R. Fuentes[2], C. A. Araujo[3]

[1] *University of Puerto Rico, Rio Piedras, PR 00936-8377*
[2] *Universidad Abierta y a Distancia, Cartagena, Colombia*
[3] *Universidad del Atlántico, Barranquilla, Colombia*

ABSTRACT

Perfect codes in the n-dimensional grid Λ_n of the lattice $\mathbb{Z}^n$ ($0 < n \in \mathbb{Z}$) and its quotient toroidal grids were obtained via the truncated distance in $\mathbb{Z}^n$ given between $u = (u_1, \cdots, u_n)$ and $v = (v_1, \ldots, v_n)$ as the graph distance $h(u, v)$ in Λ_n, if $|u_i - v_i| \leq 1$, for all $i \in \{1, \ldots, n\}$, and as $n + 1$, otherwise. Such codes are extended to superlattice graphs Γ_n obtained by glueing ternary n-cubes along their codimension 1 ternary subcubes in such a way that each binary n-subcube is contained in a unique maximal lattice of Γ_n. The existence of an infinite number of isolated perfect truncated-metric codes of radius 2 in Γ_n for $n = 2$ is ascertained, leading to conjecture such existence for $n > 2$ with radius n.

Keywords: Motzkin paths, unary-binary trees, bijection

1. Perfect truncated-metric codes

Motivated by ideas in computer architecture associated to signal transmission via a finite field (cf. [10, 9, 13]) and related with ideas in coding theory and lattice domination by means of the Lee metric arising from the Minkowsky ℓ_p norm [4] with $p = 1$, these ideas are tied to the Golomb-Welch Conjecture [12, 14, 15] investigated via perfect Lee codes [10], diameter perfect Lee codes [13], tilings with generalized Lee spheres [2, 9], perfect dominating sets (PDS's) [19], perfect-distance dominating sets (PDDS's) [1] and efficient dominating sets [8].

Let $0 < n \in \mathbb{Z}$. The aforementioned codes and dominating sets are realized in the tiling of the lattice $\mathbb{Z}^n$ whose tiles are translates of a common generalized Lee sphere. This tiling happens in the

✉ Corresponding author.
E-mail address: italo.dejter@gmail.com (I. J. Dejter).

Received 02 April 2025; Revised 30 April 2025; Accepted 29 May 2025; Published 24 June 2025.

DOI: 10.61091/jcmcc126-17

n-dimensional grid Λ_n, namely the *lattice graph* whose vertex set is $\mathbb{Z}^n$ with exactly one edge between each two vertices at euclidean distance 1. A natural follow-up here is to consider tilings of $\mathbb{Z}^n$ with two different generalized Lee spheres, which for $n > 3$ is only possible by modifying the notion of Lee distance d to that of a *truncated distance* ρ, defined below (not a standard distance, but see Remark 1.6), having perfect code applications (Subsection 1.3, based on the rainbow-coloring results of [11]).

Furthermore, *superlattice graphs* Γ_n, namely compounds of ternary n-cubes glued along codimension 1 ternary subcubes (Remark 1.1 and Section 2) that generalize the lattice graphs Λ_n (even though the Γ_n are not lattice graphs themselves), allow to extend the mentioned perfect code applications (Section 3). These graphs Γ_n can be taken as " alternate reality" graphs since they offer from each vertex of any of its ternary n-cubes glued in the compound Γ_n two ternary options as arrows indicating coordinate directions.

The *Hamming distance* $h(u, v)$ between vectors $u = (u_1, \cdots, u_n)$ and $v = (v_1, \ldots, v_n)$ in $\mathbb{Z}^n \subset \mathbb{R}^n$ is the number of positions $i \in [n] = \{1, \ldots, n\}$ for which $u_i \neq v_i$. Now, let $\rho : \mathbb{Z}^n \times \mathbb{Z}^n \to \mathbb{Z}$ be given by:

$$\rho(u, v) = \begin{cases} h(u, v), & \text{if } |u_i - v_i| \leq 1 \text{ for all } i \in [n]; \\ n + 1, & \text{otherwise.} \end{cases} \tag{1}$$

Given $S \subseteq \mathbb{Z}^n$, let $[S]$ be the induced subgraph of S in Λ_n. In (1), the Hamming distance h is equivalent to the graph distance in Λ_n, which is extensible to the graphs Γ_n. These graphs Γ_n allow the formation of algorithm flowcharts that can be adapted to follow directions in the ternary n-cubes, with vertices representing decision conditional diamonds that lead to "Yes" or "True" and "No" or "False" arrows, i.e. two oriented edges representing two sides of a triangle in a ternary $(n-1)$-cube, each such arrow representing one or more process rectangles. An elementary example of this is given in Section 4.

We assign to each component H of $[S]$ an integer $t_H > 0$ to be understood as the *radius* of a *truncated sphere with center* H. Moreover, for every component H' of $[S]$ in the translation class $\langle H \rangle$ of H in $\mathbb{Z}^n$, we assume $t_{H'} = t_H$. This yields a correspondence κ from the set of translation classes $\langle H \rangle$ of components H of $[S]$ into $\mathbb{Z}$ such that $\kappa(\langle H \rangle) = t_H$, $\forall H \in \langle H \rangle$.

Let $\rho(u, S) = \min\{\rho(u, s) | s \in S\}$. Let $(H)^{\kappa(\langle H \rangle)} = \{u \in \mathbb{Z}^n | \rho(u, H) \leq \kappa(\langle H \rangle)\}$. For each component H of S, $(H)^{\kappa(\langle H \rangle)}$ is the *truncated sphere centered at* H (or *around* H) *with radius* $\kappa(\langle H \rangle)$. Here, H is the *truncated center of* $(H)^{\kappa(\langle H \rangle)}$ and its vertices are the *central vertices of* H.

A *κ-perfect truncated-metric code*, or *κ-PTMC*, is a set $S \subseteq \mathbb{Z}^n$ such that for every $u \in \mathbb{Z}^n$ there exists a unique $s \in S$ with $\rho(u, s) = \rho(u, S)$ and such that the collection

$$\{(H)^{\kappa(\langle H \rangle)} | H \text{ is a connected component of } S\}, \tag{2}$$

forms a partition of $\mathbb{Z}^n$.

Given $0 < t \in \mathbb{Z}$, a κ-PTMC is a *t-PTMC* if all $\kappa(\langle H \rangle)$'s are equal to t. If $|H| = 1$, then $|(H)^t| = \sum_{i=0}^{t} 2^i \binom{n}{i}$, for $0 \leq t \leq n$, (which is less than the cardinal of the corresponding ℓ_1 sphere of radius t, for $t > 1$ [4]). We note that 1-PTMC's coincide with PDS's [19].

Remark 1.1. A *binary* (resp. *ternary*) *n-cube graph* Q_n^i, succinctly called *n-cube* (resp. *n-tercube*), is a cartesian product $K_i \square \cdots \square K_i$ of n complete graphs K_i with $V(K_i) = \{0, \ldots, i-1\} = F_i$, the field of order $i = 2$ (resp. 3). In Sections 2 and 3, we extend the study of PTMC's from the graphs Λ_n

to the graphs Γ_n. These cannot have non-isolated PDS's, or non-isolated 1-PTMC's. However, the ternary perfect single-error-correcting codes of length $\frac{3^t-1}{2}$ [2, 17] are isolated PDS's, that is efficient dominating sets [8] in the ternary $\frac{3^t-1}{2}$-cubes. These also are edge-disjoint unions of triangles, for $t > 0$.

In Γ_n for Sections 2 and 3, we redefine now a *non-isolated PDS* as a subset $S \subset V(\Gamma_n)$ if every vertex of Γ_n not in S is adjacent to just either one vertex of S (as in *PDS*'s) or the two end-vertices of an edge of S. As a consequence now, a non-isolated PDS is not necessarily a PDS.

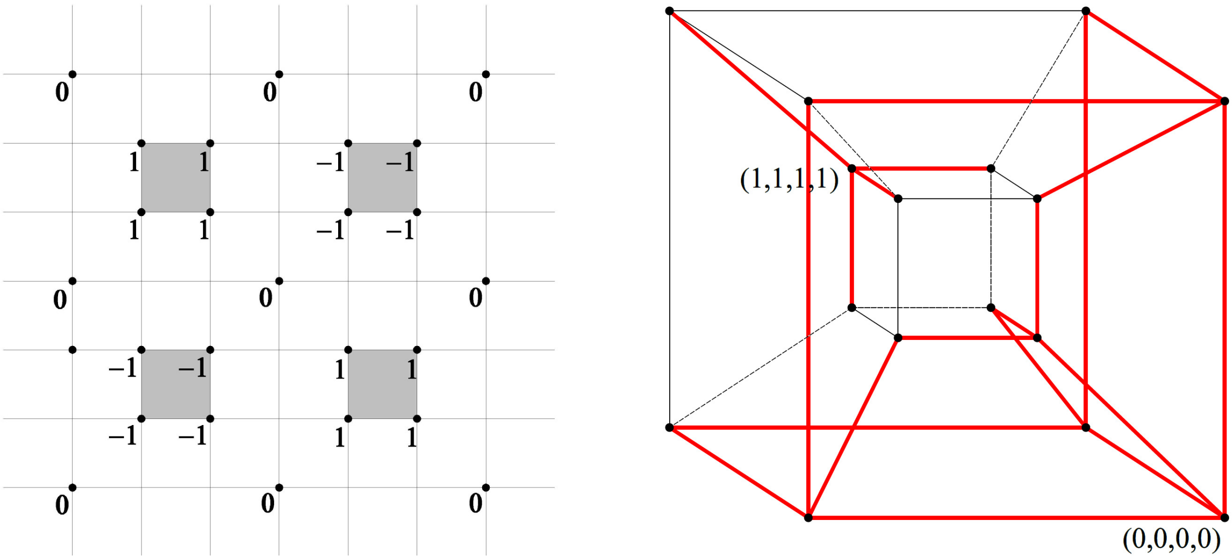

Fig. 1. Example accompanying Remark 1.2

Remark 1.2. Some graph-coloring results of [11] are restated below in Theorem 1.11-1.13 in terms of PTMC's asserting the existence of PTMC's in Λ_n that are *lattice* [13], that is *lattice-like* [1], having their induced components H with vertex sets:

(a) whose convex hulls are n-parallelotopes (resp. both 0-cubes and $(n-1)$-cubes);

(b) contained in, and dominating, truncated spheres centered at the components H of radius n (resp. radii $n-2$ and 1) that are the tiles of an associated lattice tiling of $\mathbb{Z}^n$; for $n = 3$, this is schematized on the left of Figure 1 representing the assignment of the last coordinate value mod 3 on the projection of the PTMC onto $\mathbb{Z}^{n-1}$; the case $n = 4$ (the first PTMC which is neither PDS nor PDDS) can be visualized in the same way, where the dominating edges, red colored in the copy of $Q_4^2 \subset \mathbb{Z}^4$ on the right of Figure 1 indicate truncated spheres of radius 2 and 1 centered respectively at $(0, 0, 0, 0)$ and $(1, 1, 1, 1)$.

Remark 1.3. We observe that:

(I) a t-PTMC (resp. a truncated t-sphere) of Λ_n is defined like a PDDS [1] (resp. generalized Lee sphere [9]) with ρ instead of the Lee distance d;

(II) 1-PTMC's of Λ_n (resp. truncated 1-spheres) coincide with PDS's [19] (resp. generalized Lee 1-spheres).

(III) an example [1] cited in Remark 1.10, below, justifies that our definition of PTMC above employs translation classes instead of isomorphism classes, for in such example the truncated spheres have common radius (namely 1) for both appearing translation classes, but that does not exclude the eventuality of an example with differing radii.

Remark 1.4. Related to Theorems 1.12 and 1.13 on building "lattice" κ-PTMC's whose induced components are r-cubes of different dimensions r $(0 \le r \le n)$, we have:

(A) the perfect covering codes with spheres of two different radii in Chapter 19 [5] and

(B) a negative answer [18] to a conjecture [19] claiming that the induced components of every 1-PTMC S in an n-cube Q_n^2 are all r-cubes Q_r^2 (not necessarily in the same translation class [7]), with r fixed. In fact, it was found in [18] that a 1-PTMC in Q_{13}^2 whose induced components are r-cubes Q_r^2 of two different values $r = r_1$ and $r = r_2$ exists, specifically for $r_1 = 4$ and $r_2 = 0$. This seems to be the only known counterexample to the cited conjecture [19].

1.1. *Notation, ℓ_p metrics and periodicity*

If no confusion arises, every $(a_1, \ldots, a_n) \in \mathbb{Z}^n$ is expressed as $a_1 \cdots a_n$. Let $O = 00\cdots 0$, $e_1 = 10\cdots 0$, $e_2 = 010\cdots 0$, $\ldots$, $e_{n-1} = 0\cdots 010$ and $e_n = 00\cdots 01$.

Let $z \in \mathbb{Z}^n$, let $H = (V, E)$ be a subgraph of Λ_n and let $H + z$ be the subgraph $H' = (V', E')$ whose vertex set is $V' = V + z = \{w \in \mathbb{Z}^n; \exists\ v \in V$ such that $w = v + z\}$ so that $uv \in E \Leftrightarrow (u+z)(v+z) \in E'$. For example, let H be induced in Λ_n by the vertices with entries in $\{0, 1\}$. Then, every translation $H + z$ of H in Λ_n (in particular H itself) is isomorphic to Q_n^2.

Let $i \in [n]$. Each edge (resp. segment) uv of Λ_n (resp. $\mathbb{R}^n \supset \mathbb{Z}^n$) with $u \neq v$ is *parallel* to $Oe_i \in E(\Lambda_n) \Leftrightarrow u - v \in \{\pm e_i\}$ (resp. $\Leftrightarrow \exists a \in \mathbb{R} \setminus \{0\}$ with $u - v = ae_i$). A *parallelotope* $\mathscr{P}$ in $\mathbb{R}^n$ is a cartesian product of segments parallel to some of the Oe_i's $(i \in [n])$. We restrict to parallelotopes $\mathscr{P}$ having their vertices in $\mathbb{Z}^n$. An *edge* of $\mathscr{P}$ is a segment of unit length parallel to some Oe_i $(i \in [n])$ separating a pair of vertices of Λ_n in $\mathscr{P}$. Recall that a *trivial* subgraph of Λ_n is composed by just one vertex. The proof of the following is similar to that of Theorem 1 [1].

Theorem 1.5. *Let $0 < t \in \mathbb{Z}$. If S is a t-PTMC in Λ_n, then the convex hull in $\mathbb{R}^n$ of the vertex set $V(H)$ of each nontrivial component H of $[S]$ is a parallelotope in $\mathbb{R}^n$ whose edges are parallel to some or all of the segments Oe_i in $E(\Lambda_n)$, where $i \in [n]$.*

Let H be a nontrivial induced subgraph of Λ_n with the convex hull of $V(H)$ in $\mathbb{R}^n$ as a parallelotope whose edges are parallel to some or all of the segments Oe_i in $E(\Lambda_n)$, $(i \in [n])$. If exactly r elements of $[n]$ are such values of i, then we say that H is an *r-box*. Note that H is a cartesian product $\Pi_{i=1}^n P^i$, where P^i is a finite path, $\forall i \in [n]$, with exactly r paths P^i having positive length.

Let $W_{n,H,t}$ be the truncated sphere of radius t around an H as above, where $0 \le t \in \mathbb{Z}$. Then, H is the truncated center of $W_{n,H,t}$. A t-PTMC S of Λ_n determines a partition of $\mathbb{Z}^n$ into spheres $W_{n,H,t}$ with H running over the components of $[S]$. Such an S with the components of $[S]$ obtained by translations from a fixed finite graph H is said to be a *t-PTMC$[H]$*. (This imitates the definition of a t-PDDS$[H]$ in [1], mentioned in Remark 1.3(I) above). Let S be a t-PTMC$[H]$ and let H' be a component of $[S]$ obtained from H by means of a translation. Then S is said to be a *lattice t-PTMC$[H]$* if and only if there is a lattice $L \subseteq \mathbb{Z}^n$ such that: H'' is a component of $[S] \Leftrightarrow H'' = H' + z$, for some $z \in L$.

Remark 1.6. It is relevant to note the connections of ρ and the ℓ_p metrics [4]: A truncated sphere of truncated radius 1 centered at some vertex v is a Lee $(p = 1)$ sphere of radius 1, whereas a truncated sphere of truncated radius n centered at v is a sphere of radius 1 in the maximum $(p = \infty)$

distance, namely $W_{n,\{v\},1}$ (which has an n-dimensional cube for convex hull). Thus, all truncated spheres in this work are spheres in some ℓ_p metric, and the truncated metrics are a convenient way to consider different ℓ_p metrics for the graph components. This observation allows connections with other previous works such as (for just one t) perfect codes in the maximum metric and in the ℓ_p metrics [4].

Remark 1.7. We start to rephrase the graph-coloring facts of [11], to be completed in Subsection 1.3. Announced as Theorem 1.11 below, there is a construction of lattice n-PTMC's S whose induced subgraphs $[S]$ in Λ_n have their components H with:

(i) vertex sets $V(H)$ whose convex hulls are n-boxes in $\mathbb{R}^n$ with distance 3 to $[S]\setminus H$, and representatives (one per component H) forming a lattice with generators along the coordinate directions;

(ii) each $V(H)$ contained in a truncated sphere $(H)^{\kappa(\langle H\rangle)}$ whose radius is n.

(We do not know whether similar lattice t-PTMC's S exist with $[S]$ having r-parallelotopes as their components, for r fixed such that $0<r<n$.)

Extending the meaning of the adjective *lattice* in Subsection 1.2 below, as in [11] we have in Theorems 1.12 and 1.13 that a lattice κ-PTMC S exists in Λ_n whose induced subgraph $[S]$ has its components H with vertex sets $V(H)$:

(i′) having both $(n-1)$-cubes and 0-cubes as their convex hulls in $\mathbb{R}^n$;

(ii′) contained in truncated spheres $(H)^{\kappa(\langle H\rangle)}$ whose radii, namely 1 and $(n-2)$, correspond respectively to the $(n-1)$-cubes and 0-cubes in item (i′).

A set $S\subset\mathbb{Z}^n=E(\Lambda_n)$ is *periodic* if and only if there exist $p_1,\dots,p_n$ in $\mathbb{Z}$ such that $v\in S$ implies $v\pm p_ie_i\in S,\forall i\in[n]$. Since each lattice t-PTMC$[H]$ S is periodic [1], then every canonical projection from Λ_n onto a toroidal grid $\mathscr{T}$, i.e. a cartesian product $\mathscr{T}=C_{k_1p_1}\square C_{k_2p_2}\square\cdots\square C_{k_np_n}$ of n cycles $C_{k_ip_i}$ $(0<k_i\in\mathbb{Z},\forall i\in[n])$, takes S onto a t-PTMC$[H]$ in $\mathscr{T}$. This observation adapts to respective situations that complement the statements of Theorems 1.11-1.13 via canonical projections from $\mathbb{Z}^n$ onto adequate toroidal grids $\mathscr{T}$.

Question 1.8. *Do lattice t-PTMC's S exist with $[S]$ having r-parallelotopes as their components, for r fixed such that $0<r<n$?*

1.2. Further specifications

Given a lattice L in $\mathbb{Z}^n$, a subset $T\subseteq\mathbb{Z}^n$ that contains exactly one vertex in each class mod L (so that T is a complete system of coset representatives of L in Λ_n) is said to be an *FR* (acronym suggesting "fundamental region") of L. A partition of $\mathbb{Z}^n$ into FR's of L is said to be a *tiling* of $\mathbb{Z}^n$. Those FR's are said to be its *tiles*.

We extend the notion of lattice κ-PTMC so that the associated *fundamental region* (see [3], pg 26), or FR (see above) of every new lattice contains a finite number of (in our applications, just two) members H of each $\langle H\rangle$.

In the literature, existing constructions of lattice t-PTMC's in Λ_n $(t<n)$ concern just $t=1$ (see [1, 2, 9, 13]) but there are not many known lattice 1-PTMC's. For example, [8] shows that there is only one lattice 1-PTMC$[Q_2^2]$ and no non-lattice 1-PTMC$[Q_2^2]$. In addition, there is a lattice 2-PDDS$[Q_1^2]$ in Λ_3 arising from a tiling of Minkowsky cited in [1].

Conjecture 1.9. *There is no* t-PTMC *lattice in Λ_n, for $1<t<n$.*

This conjecture has an analogous form for perfect codes in the ℓ_p metrics in [4], and together with the conjecture mentioned in Remark 1.4(B), produces a contrast with the constructions in Theorems 1.12 and 1.13, below.

If S is a periodic non-lattice t-PTMC$[H]$ in Λ_n, then there exists $0 < m \in \mathbb{Z}$ and a tiling of Λ_n with tiles that are disjoint copies of the vertex set $V(H^*)$ of a connected subgraph H^* induced in Λ_n by the union of:

(a) the vertex sets of m disjoint copies $H^1, \dots, H^m$ of H (components of $[S]$);

(b) the sets $(H^j)^{\kappa(\langle H\rangle)}$ of vertices $v \in \mathbb{Z}^n$ with $\rho(v, H^j) \le t$, for $j \in [m]$, where $(H^1)^{\kappa(\langle H\rangle)}, \dots, (H^m)^{\kappa(\langle H\rangle)}$ are pairwise disjoint copies of $(H)^{\kappa(\langle H\rangle)}$ in $\mathbb{Z}^n$.

By taking such an m as small as possible, we say that S is a *t-PTMC$[H;m]$*.

Remark 1.10. In Section 5 [1], a non-lattice 1-PTMC$[Q_1^2;4]$ S is shown to exist with a lattice L_S based on it, each of the FR's of L_S containing two copies of Q_2^2 parallel to Oe_1 and two more copies of Q_2^2 parallel to Oe_2, these four copies being components of $[S]$, namely generated say by the vertices $(1,0)$, $(2,0)$, $(1,3)$, $(2,3)$, $(0,1)$, $(0,2)$, $(3,1)$ and $(3,2)$.

Thus, even for a non-lattice t-PTMC S in a Λ_n, a lattice can be recovered and formed by selected vertices v_T in the corresponding tiles T associated with S. We say that such set S is a *lattice t-PTMC$[H;m]$*, indicating the number m of isomorphic components of $[S]$ in a typical tile T in which to fix a distinguished vertex v_T.

We further specify the developments above as follows. A t-PTMC S in Λ_n with the components of $[S]$ obtained by translations from two non-parallel subgraphs H_0, H_1 of Λ_n is said to be a *t-PTMC$[H_0, H_1]$*. The case of this in Remark 1.10 is a κ-PTMC, with two translation classes of components of $[S]$ formed by the copies of Q_2^2 parallel to each of the directions coordinates. Here, κ sends those copies onto $t = 1$. Each tile of this κ-PTMC contains two copies of Q_2^2 parallel to Oe_1 and two copies of Q_2^2 parallel to Oe_2, accounting for $m = 4$.

More generally, let $t_i \in [n]$, for $i = 0, 1$. We say that a set $S \subset V$ is a *(t_0, t_1)-PTMC$[H_0, H_1]$* in Λ_n if for each $v \in V$ there is:

(i$''$) a unique index $i \in \{0, 1\}$ and a unique component H_v^i of $[S]$ obtained by means of a translation from H_i such that the truncated distance $\rho(v, H_v^i)$ from v to H_v^i satisfies $\rho(v, H_v^i) \le t_i$ and

(ii$''$) a unique vertex w in H_v^i such that $\rho(v, w) = \rho(v, H_v^i)$.

Even though such a set S is not lattice as in [13] (or lattice-like [1]), it may happen that there exists a lattice $L_S \subset \mathbb{Z}^n$ such that for $0 < m_0, m_1 \in \mathbb{Z}$ there exists an FR of L_S in Λ_n given by the union of two disjoint subgraphs H_0^*, H_1^*, where H_i^* $(i = 0, 1)$ is induced in Λ_n by the disjoint union of:

(a$'$) the vertex sets of m_i disjoint copies $H_i^1, \dots, H_i^{m_i}$ of H_i, (components of $[S]$);

(b$'$) the sets $(H_i^j)^{\kappa(\langle H\rangle)}$ of vertices $v \in \mathbb{Z}^n$ for which $0 < \rho(v, H_i^j) \le t_i$, for $j \in [m_i]$, where $(H_i^1)^{\kappa(\langle H\rangle)}, \dots, (H_i^{m_i})^{\kappa(\langle H\rangle)}$ are pairwise disjoint copies of $H^\kappa(\langle H\rangle))$ in $\mathbb{Z}^n$.

1.3. *Restatement of graph-coloring results*

A particular case of lattice t-PTMC$[H]$ is that in which H is an n-box of Λ_n. For each such H, Theorem 1.11 below says that there is a lattice n-PTMC$[H]$ in Λ_n. (In [2], n-boxes of unit volume in Λ_n are shown to determine 1-PDDS$[H]$'s if and only if either $n = 2^r - 1$ or $n = 3^r - 1$).

From Subsection 1.1 we know that S determines a partition of $\mathbb{Z}^n$ into spheres $W_{n,H',n}$, where H' runs over the components of $[S[$. In each $W_{n,H',n}$, let $b_1 b_2 \cdots b_n$ be the vertex $a_1 a_2 \cdots a_n$ for which

$a_1 + a_2 + \cdots + a_n$ is minimal. We say that this $b_1b_2\cdots b_n$ is the *anchor* of $W_{n,H',n}$. The anchors of the spheres $W_{n,H',n}$ form the lattice $L = L_S$. Without loss of generality we can assume that O is the anchor of a $W_{n,H_0,n}$ whose truncated center H_0 is a component of $[S]$. Let $c_1c_2\cdots c_n$ be the vertex $a_1a_2\cdots a_n$ in $W_{n,H_0,n}$ for which $a_1 + a_2 + \cdots + a_n$ is maximal. Then L_S has generating set $\{(1+c_1)e_1, (1+c_2)e_2, \ldots, (1+c_n)e_n\}$ and is formed by all linear combinations of those $(1+c_i)e_i$, $(i \in [n])$.

Theorem 1.11. [11] *For each $i \in [n]$, let P_i be a path of length $c_i - 2$, parallel to Oe_i, and let $H = \Pi_{i=1}^n P_i$ be an n-box in Λ_n. Then, there is a lattice n-PTMC$[H]$ S of Λ_n with minimum ℓ_1-distance 3 between the components of $[S]$.*

Theorem 1.12. [11] *There exists a lattice* 1-PTMC$[Q_2^2, Q_0^2; 2, 2]$ *(in particular a* PDS*) S in Λ_3 with minimum ℓ_1-distance 3 between the components of $[S]$.*

To state Theorem 1.13, let $H_0 = Q_{n-1}^2$, $H_1 = Q_0^2$, $m_0 = m_1 = 2$, $t_0 = 1$, $t_1 = n-2$.

Theorem 1.13. *There exists a lattice* $(1, n-2)$-PTMC$[Q_{n-1}^2, Q_0^2; 2, 2]$ *S in Λ_n.*

Remark 1.14. From the last observation in Remark 1.7, (just before Question 1.8), it can be deduced that the respective PTMC S covers (via canonical projections) in Theorems 1.11, 1.12 and 1.13, respectively:

- an n-PTMC$[H]$ in $\mathscr{T} = C_{c_1k_1}\Box C_{c_2k_2}\Box\cdots\Box C_{c_nk_n}, (1 < k_i \in \mathbb{Z}, \forall i \in [n])$;
- a 1-PTMC$[Q_2^2, Q_0^2; 2, 2]$ in $\mathscr{T} = C_{6k_1}\Box C_{6k_2}\Box C_{3k_3}, (0 < k_i, \forall i \in [3])$;
- a $(1, n-2)$-PTMC$[Q_{n-1}^2, Q_0^2; 2, 2]$ in $\mathscr{T} = C_{6k_1}\Box\ldots\Box C_{6k_{n-1}}\Box C_{3k_n}, (0 < k_i, \forall i \in [n])$.

2. Ternary superlattice graphs

Let the 2-tercube, or *tersquare*, Q_2^3 be denoted $[\emptyset]$, with vertices given by the 2-tuples xy, $(x, y \in F_3 = \{0,1,2\})$. As a graph, $[\emptyset] = (0,1,2)\Box(0,1,2)$, namely the cartesian product of two triangles whose vertex sets are both F_3, is represented at the center of Figure 2 sharing a triangle with each one of 15 tersquares, to be specified below, in respective partially viewable colored backgrounds. The *1-sub-tercubes* or *triangles* Q_1^3 of the 2-tercube $[\emptyset]$ have vertex sets $\{0y\}_{y\in F_3}$, $\{1y\}_{y\in F_3}$, $\{2y\}_{y\in F_3}$, $\{x0\}_{x\in F_3}$, $\{x1\}_{x\in F_3}$, $\{x2\}_{x\in F_3}$. They will be indicated x^0, x^1, x^2, y^0, y^1, y^2, respectively. To each of these triangles t^s $(t \in \{x,y\}; s \in F_3)$ of $[\emptyset]$ we glue a corresponding tersquare $[{t \atop s}]$ intersecting $[\emptyset]$ exactly in t^s.

This way, six tersquares $[{x \atop 0}], \ldots, [{y \atop 2}]$ are obtained (to be called *subcentral tersquares*, colored yellow and light-blue in Figure 2) that intersect $[\emptyset]$ respectively in the triangles $x^0, \ldots, y^2$. Next, we glue to the remaining new triangles (i.e., other than those already in $[\emptyset]$), a set of nine new tersquares that we denote $[{xy \atop 00}], \ldots, [{xy \atop 22}]$ (and call *corner tersquares*, colored green and gray in Figure 2). These nine tersquares share merely a vertex with $[\emptyset]$ and their disposition with respect to the central tersquare $[\emptyset]$ and subcentral tersquares $x^0, \ldots, y^2$ is specified in Figure 2. In fact, $[{xy \atop ij}]$ shares a triangle y^j with $[{x \atop i}]$ and a triangle x^i with $[{y \atop j}]$, for $i, j = 0, 1, 2$. Such triangles can be further specified respectively as $y^j[{x \atop i}]$ and $x^i[{y \atop j}]$.

The graph $[[\emptyset]]$ resulting from the union of the $1+6+9 = 16$ tersquares constructed so far, will be referred to as the 2-*hive* $[[\emptyset]]$. The *central tersquare* $[\emptyset]$ of $[[\emptyset]]$ shares just one triangle with each of the six subcentral tercubes and just one vertex with each of the nine corner tersquares. The tersquare $[\emptyset]$, given as a subgraph at the center of Figure 2, also results in the representation at the lower-right quarter of Table 1 by identifying the quadruple of vertices labelled 22, as well as each pair of vertices labelled 20, 21, 02 and 12.

Table 1.

$\begin{array}{ccccccccccc} 01 & - & 11 & - & 01 & - & 11 & - & 01 & - & 11 \\ \vert & \begin{bmatrix}xxyy\\0110\end{bmatrix} & \vert & \begin{bmatrix}xyy\\010\end{bmatrix} & \vert & \begin{bmatrix}yy\\10\end{bmatrix} & \vert & \begin{bmatrix}xyy\\110\end{bmatrix} & \vert & \begin{bmatrix}xxyy\\1010\end{bmatrix} & \vert \\ 00 & - & 10 & - & 00 & - & 10 & - & 00 & - & 10 \\ \vert & \begin{bmatrix}xxy\\011\end{bmatrix} & \vert & \begin{bmatrix}xy\\01\end{bmatrix} & \vert & \begin{bmatrix}y\\1\end{bmatrix} & \vert & \begin{bmatrix}xy\\11\end{bmatrix} & \vert & \begin{bmatrix}xxy\\101\end{bmatrix} & \vert \\ 01 & - & 11 & - & 01 & - & 11 & - & 01 & - & 11 \\ \vert & \begin{bmatrix}xx\\01\end{bmatrix} & \vert & \begin{bmatrix}x\\0\end{bmatrix} & \vert & [\emptyset] & \vert & \begin{bmatrix}x\\1\end{bmatrix} & \vert & \begin{bmatrix}xx\\10\end{bmatrix} & \vert \\ 00 & - & 10 & - & 00 & - & 10 & - & 00 & - & 10 \\ \vert & \begin{bmatrix}xxy\\010\end{bmatrix} & \vert & \begin{bmatrix}xy\\00\end{bmatrix} & \vert & \begin{bmatrix}y\\0\end{bmatrix} & \vert & \begin{bmatrix}xy\\10\end{bmatrix} & \vert & \begin{bmatrix}xxy\\100\end{bmatrix} & \vert \\ 10 & - & 11 & - & 10 & - & 11 & - & 10 & - & 11 \\ \vert & \begin{bmatrix}xxyy\\0101\end{bmatrix} & \vert & \begin{bmatrix}xyy\\001\end{bmatrix} & \vert & \begin{bmatrix}yy\\01\end{bmatrix} & \vert & \begin{bmatrix}xyy\\101\end{bmatrix} & \vert & \begin{bmatrix}xxyy\\1001\end{bmatrix} & \vert \\ 00 & - & 01 & - & 00 & - & 01 & - & 00 & - & 01 \end{array}$	$\begin{array}{ccccccccccc} 02 & - & 22 & - & 02 & - & 22 & - & 02 & - & 22 \\ \vert & \begin{bmatrix}xxyy\\0220\end{bmatrix} & \vert & \begin{bmatrix}xyy\\020\end{bmatrix} & \vert & \begin{bmatrix}yy\\20\end{bmatrix} & \vert & \begin{bmatrix}xyy\\220\end{bmatrix} & \vert & \begin{bmatrix}xxyy\\2020\end{bmatrix} & \vert \\ 00 & - & 20 & - & 00 & - & 20 & - & 00 & - & 20 \\ \vert & \begin{bmatrix}xxy\\022\end{bmatrix} & \vert & \begin{bmatrix}xy\\02\end{bmatrix} & \vert & \begin{bmatrix}y\\2\end{bmatrix} & \vert & \begin{bmatrix}xy\\22\end{bmatrix} & \vert & \begin{bmatrix}xxy\\202\end{bmatrix} & \vert \\ 02 & - & 22 & - & 02 & - & 22 & - & 02 & - & 22 \\ \vert & \begin{bmatrix}xx\\02\end{bmatrix} & \vert & \begin{bmatrix}x\\0\end{bmatrix} & \vert & [\emptyset] & \vert & \begin{bmatrix}x\\2\end{bmatrix} & \vert & \begin{bmatrix}xx\\20\end{bmatrix} & \vert \\ 00 & - & 20 & - & 00 & - & 20 & - & 00 & - & 20 \\ \vert & \begin{bmatrix}xxy\\020\end{bmatrix} & \vert & \begin{bmatrix}xy\\00\end{bmatrix} & \vert & \begin{bmatrix}y\\0\end{bmatrix} & \vert & \begin{bmatrix}xy\\20\end{bmatrix} & \vert & \begin{bmatrix}xxy\\200\end{bmatrix} & \vert \\ 20 & - & 22 & - & 20 & - & 22 & - & 20 & - & 22 \\ \vert & \begin{bmatrix}xxyy\\0202\end{bmatrix} & \vert & \begin{bmatrix}xyy\\002\end{bmatrix} & \vert & \begin{bmatrix}yy\\02\end{bmatrix} & \vert & \begin{bmatrix}xyy\\202\end{bmatrix} & \vert & \begin{bmatrix}xxyy\\2002\end{bmatrix} & \vert \\ 00 & - & 02 & - & 00 & - & 02 & - & 00 & - & 02 \end{array}$
$\begin{array}{ccccccccccc} 12 & - & 22 & - & 12 & - & 22 & - & 12 & - & 22 \\ \vert & \begin{bmatrix}xxyy\\1221\end{bmatrix} & \vert & \begin{bmatrix}xyy\\121\end{bmatrix} & \vert & \begin{bmatrix}yy\\21\end{bmatrix} & \vert & \begin{bmatrix}xyy\\221\end{bmatrix} & \vert & \begin{bmatrix}xxyy\\2121\end{bmatrix} & \vert \\ 11 & - & 21 & - & 11 & - & 21 & - & 11 & - & 21 \\ \vert & \begin{bmatrix}xxy\\122\end{bmatrix} & \vert & \begin{bmatrix}xy\\12\end{bmatrix} & \vert & \begin{bmatrix}y\\2\end{bmatrix} & \vert & \begin{bmatrix}xy\\22\end{bmatrix} & \vert & \begin{bmatrix}xxy\\212\end{bmatrix} & \vert \\ 12 & - & 22 & - & 12 & - & 22 & - & 12 & - & 22 \\ \vert & \begin{bmatrix}xx\\12\end{bmatrix} & \vert & \begin{bmatrix}x\\1\end{bmatrix} & \vert & [\emptyset] & \vert & \begin{bmatrix}x\\2\end{bmatrix} & \vert & \begin{bmatrix}xx\\21\end{bmatrix} & \vert \\ 11 & - & 21 & - & 11 & - & 21 & - & 11 & - & 21 \\ \vert & \begin{bmatrix}xxy\\121\end{bmatrix} & \vert & \begin{bmatrix}xy\\11\end{bmatrix} & \vert & \begin{bmatrix}y\\1\end{bmatrix} & \vert & \begin{bmatrix}xy\\21\end{bmatrix} & \vert & \begin{bmatrix}xxy\\211\end{bmatrix} & \vert \\ 12 & - & 22 & - & 12 & - & 22 & - & 12 & - & 22 \\ \vert & \begin{bmatrix}xxyy\\1212\end{bmatrix} & \vert & \begin{bmatrix}xyy\\112\end{bmatrix} & \vert & \begin{bmatrix}xy\\12\end{bmatrix} & \vert & \begin{bmatrix}xyy\\212\end{bmatrix} & \vert & \begin{bmatrix}xxyy\\2112\end{bmatrix} & \vert \\ 11 & - & 21 & - & 11 & - & 21 & - & 11 & - & 21 \end{array}$	$\begin{array}{ccccccc} 22 & - & 02 & - & 12 & - & 22 \\ \vert & & \vert & & \vert & & \vert \\ 21 & - & 01 & - & 11 & - & 21 \\ \vert & & \vert & [\emptyset] & \vert & & \vert \\ 20 & - & 00 & - & 10 & - & 20 \\ \vert & & \vert & & \vert & & \vert \\ 22 & - & 02 & - & 12 & - & 22 \end{array}$

The construction above continues with the iterative glueing of tersquares along *free* triangles, namely those triangles along which glueing of a new continuing tersquare was not already performed. In the limit of feasible glueings, a total compound graph Γ_2 of tersquares, glued in pairs of adjacent tersquares along corresponding triangles, results in an infinite locally finite graph, the *ternary square compound* graph Γ_2, that we also call *ternary non-lattice superlattice graph.* Notation for all tersquares and triangles of Γ_2, continuing the notation of the 16 tersquares and their triangles above, is completed below. The word "superlattice" here corresponds to the fact that, even though Γ_n is not a lattice graph itself, it is such that each of its binary n-cubes is contained in a unique maximal lattice of Γ_n.

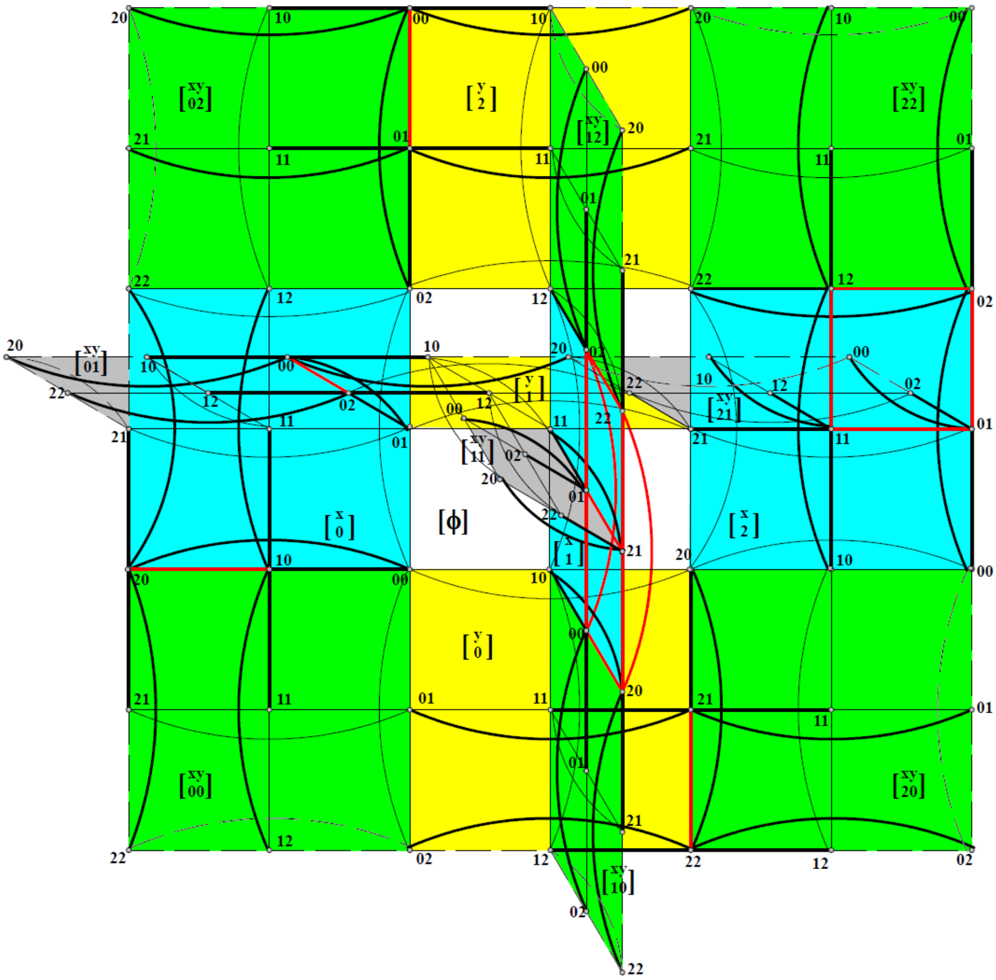

Fig. 2. Representing a PDS of $[[\emptyset]]$ in Γ_2

Three subgraphs of Γ_2 are represented in Table 1, containing just one 4-cycle (of the 9 in Q_2^3) per participating (but not totally shown) glued tersquare. This yields 9 sub-lattice types in Γ_2 (one per 4-cycle of Q_2^3, three partially shown in Table 1), each isomorphic to Λ_2. Thus, Γ_2 is a superset of each of the copies of Λ_2 generated by some 4-cycle of Γ_2. We further specify Γ_2 after presenting a non-isolated PDS in $[[\emptyset]]$ (Theorem 2.1).

The large connected graph in Figure 2 represents the 2-hive $[[\emptyset]]$, with $[\begin{smallmatrix}x\\0\end{smallmatrix}]$, $[\begin{smallmatrix}x\\1\end{smallmatrix}]$ and $[\begin{smallmatrix}x\\2\end{smallmatrix}]$ in light-blue background, $[\begin{smallmatrix}y\\0\end{smallmatrix}]$, $[\begin{smallmatrix}y\\1\end{smallmatrix}]$ and $[\begin{smallmatrix}x\\2\end{smallmatrix}]$ in yellow background, and the nine tersquares $[\begin{smallmatrix}xy\\ij\end{smallmatrix}]$ in green background if $y \neq 1$ and light-gray background if $y = 1$, where the apparent colored areas spatial disposition results in the partial hiding of some of these areas. The thick red edges induce a subgraph of $[[\emptyset]]$ whose vertex set is a non-isolated PDS S (as defined in Remark 1.1) of $[[\emptyset]]$. The dominating edges are drawn in thick black trace, allowing the reader to verify that all vertices of $[[\emptyset]]$ not in S are dominated as indicated in Remark 1.1. (It is elementary to verify that no isolated PDS in $[[\emptyset]]$ exists). The remaining edges of $[[\emptyset]]$, not in thick trace, are in dashed trace if they are "exterior" edges of $[[\emptyset]]$ (i.e., those shared by 2-hives other than $[[\emptyset]]$ in Γ_2) and in thin trace otherwise (i.e., if they are "interior" edges of $[[\emptyset]]$). Motivation for pursuing such a non-isolated PDS arose as a palliative remedy for the impossibility of having here a PDS like the Livingston-Stout PDS in the grid $P_4\Box P_4$ [16], which happens to be the only isolated PDS in grid graphs $P_m\Box P_n$, for $2 < min\{m,n\}$ [6].

Theorem 2.1. *There exists a non-isolated PDS, or 1-PTMC*$[Q_1^2, Q_2^2, Q_1^3\square Q_1^2; 4, 1, 1]$, *in the 2-hive* $[[\emptyset]] \subset \Gamma_2$.

Proof. The claimed PDS in $[[\emptyset]]$ is formed by the vertex sets of the following components (of its induced subgraphs):

(a) the edge $(00, 01)$ of triangle $(00, 01, 02)$ shared by tersquares $[{}^{y}_{2}]$ and $[{}^{xy}_{02}]$;

(b) the edge $(10, 20)$ of triangle $(00, 10, 20)$ shared by tersquares $[{}^{x}_{0}]$ and $[{}^{xy}_{00}]$;

(c) the edge $(21, 22)$ of triangle $(20, 21, 22)$ shared by tersquares $[{}^{y}_{0}]$ and $[{}^{xy}_{20}]$;

(d) the edge $(00, 02)$ of triangle $(00, 02, 01)$ shared by tersquares $[{}^{y}_{1}]$ and $[{}^{xy}_{01}]$;

(e) the 4-cycle $(02, 12, 11, 01)$ of tersquare $[{}^{x}_{2}]$, where its edge $(02, 12)$ (of triangle $\Delta = (02, 12, 22)$) is shared (with Δ) with tersquare $[{}^{xy}_{22}]$;

(f) the triangular prism in $[{}^{x}_{1}]$ formed by triangles $(00, 01, 02)$ and $(20, 21, 22)$ and edges $(00, 20)$, $(02, 22)$ (of triangle $(02, 22, 12)$, shared by tersquare $[{}^{xy}_{22}]$) and $(01, 21)$ (of triangle $(01, 21, 11)$, shared by tersquare $[{}^{xy}_{11}]$).

As can be verified in Figure 2, the edges departing from these red-edge components cover all other vertices of $[[\emptyset]]$, proving the theorem. $\square$

Figure 2 may be augmented by adding the tersquares $[{}^{xx\,y}_{i\,j\,k}]$, with $i \neq j$ in F_3, etc. One may continue by adding tersquares $[{}^{xx\cdots xx\,yy\cdots yy}_{i\,j\,\cdots kl\,mn\cdots pq}]$ with $i \neq j \neq \ldots \neq k \neq l$ (resp. $m \neq n \neq \ldots \neq p \neq q$), i.e. not two contiguous equal values under the x's (resp. y's). Taking $i, j, \ldots, k, l, m, n, \ldots p, q$ in F_3 to be contiguously different with just two values, (e.g. 0,1; resp. 0,2; resp. 1,2, in the upper-left; resp. upper-right; resp. lower-left quarter in Table 1) is a way of obtaining 3 sub-lattices of Γ_2, each isomorphic to Λ_2, as in Table 1. But there is an infinite family of "parallel" sub-lattices in Γ_2 for each of the 9 sublattice types, one per each 4-cycle of a typical tersquare as in the lower-left quarter of Table 1. For example, the type with values 0,2 represents "parallel" sub-lattices having "shortest" tersquares $[\emptyset]$, $[{}^{x}_{1}]$, $[{}^{y}_{1}]$, $[{}^{xx}_{01}]$, $[{}^{yy}_{01}]$, $[{}^{xx}_{21}]$, $[{}^{yy}_{21}]$, etc., including every $[{}^{xx\cdots xx}_{i\,j\,\cdots kl}]$, $[{}^{y\,y\cdots y\,y}_{mn\cdots pq}]$ and $[{}^{xx\cdots xx\,yy\cdots yy}_{i\,j\,\cdots kl\,mn\cdots pq}]$.

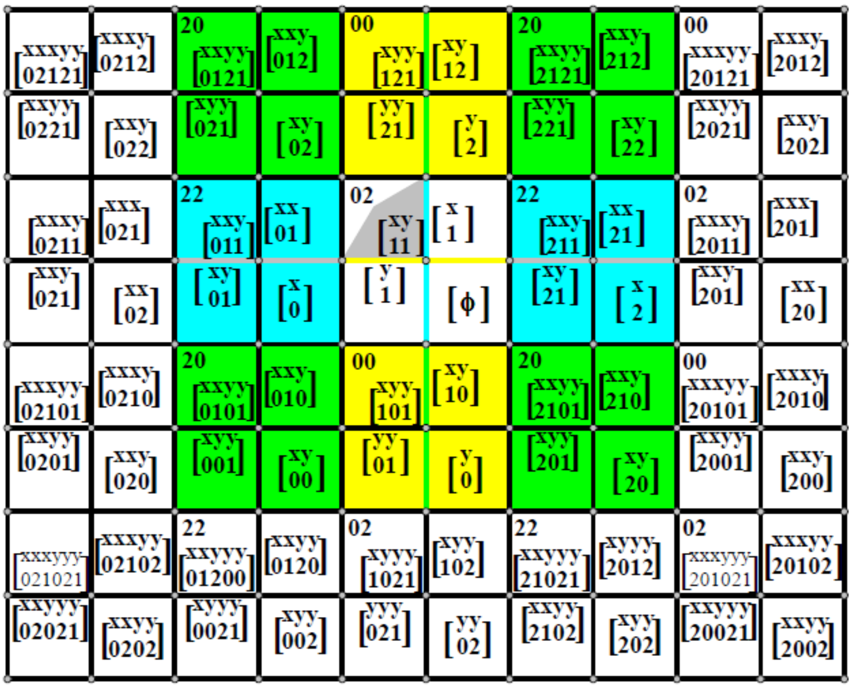

Fig. 3. Planar projection of a portion of Γ_2 larger than in Figure 2

These sub-lattices can be refined by replacing each edge e in them by the 2-path closing a triangle with e and adding more vertices and additional edges out of them to the new vertices obtained by the said replacement, in order to distinguish the glued 2-tercubes in Γ_2. In particular, Figure 2 is obtained from such a procedure by starting from a plane containing the upper-right quarter of Table 1. Figure 3 shows a projection of a partial extension of Figure 2 in such a plane, where tersquare colors are kept as in Figure 2, including if they are projected into a 2-path. Colors here still are light-blue, blue, green and light-gray. Each tersquare in Figure 3, represented by four squares with the common central vertex 11, is just recognizable by its upper-left vertex denomination presence. Of the four such squares, the lower-right one has the corresponding tersquare denomination. The other tersquare denominations in the three remaining squares correspond to the counterpart denominations in the representation of $[\emptyset]$.

Definition 2.2. A *ternary n-cube compound* graph Γ_n is defined as the union of all necessary n-tercubes that appeared glued along their (codimension 1) ternary $(n-1)$-subtercubes, for any $2 < n \in \mathbb{Z}$. The vertices of such Γ_n are given in terms of the n-tercubes. These, that can be denoted

$$\left[\begin{smallmatrix}x\\0\end{smallmatrix}\right], \left[\begin{smallmatrix}y\\0\end{smallmatrix}\right], \dots, \left[\begin{smallmatrix}z\\0\end{smallmatrix}\right], \left[\begin{smallmatrix}x\\1\end{smallmatrix}\right], \left[\begin{smallmatrix}y\\1\end{smallmatrix}\right], \dots, \left[\begin{smallmatrix}z\\1\end{smallmatrix}\right], \left[\begin{smallmatrix}x\\2\end{smallmatrix}\right], \left[\begin{smallmatrix}y\\2\end{smallmatrix}\right], \dots, \left[\begin{smallmatrix}z\\2\end{smallmatrix}\right], \left[\begin{smallmatrix}xy\\00\end{smallmatrix}\right], \dots,$$

including all those of the general form $[J] = \left[\begin{smallmatrix}xx\cdots xx\, yy\cdots yy \,\cdots\cdots\, zz\cdots zz\\ i\,j\,\cdots kl\, mn\cdots pq \,\cdots\cdots\, rs\cdots vw\end{smallmatrix}\right]$, where $x, y, \dots, z$ represent the n (ternary) coordinate directions. Such n-tercubes are assigned locally by reflection on the $(n-1)$-subtercubes. Thus the said vertices can be denoted $x^0[J], \dots, z^2[J]$, by following the notations above.

Example 2.3. Figure 2 for $n = 2$, represents the 2-hive $[[\emptyset]]$ with $[\emptyset]$ at its center, and its neighboring tersquares $\left[\begin{smallmatrix}x\\0\end{smallmatrix}\right]$, $\left[\begin{smallmatrix}x\\1\end{smallmatrix}\right]$, $\left[\begin{smallmatrix}x\\2\end{smallmatrix}\right]$ in light-blue background, $\left[\begin{smallmatrix}y\\0\end{smallmatrix}\right]$, and $\left[\begin{smallmatrix}y\\1\end{smallmatrix}\right]$, $\left[\begin{smallmatrix}y\\2\end{smallmatrix}\right]$ in yellow background, and the tersquares neighboring those tersquares, namely $\left[\begin{smallmatrix}xy\\i\,j\end{smallmatrix}\right]$, $(i, j \in F_3)$, in green and light-gray backgrounds. It can be seen that Γ_n may be considered as a superset of Λ_n in three different ways, as was commented above in relation to Table 1 for $n = 2$.

We pose the following.

Question 2.4. *Does there exist a non-isolated PDS S in Γ_n, for $n \geq 2$? If so, could S behave like a lattice, for example by restricting itself to a lattice PDS over any sub-lattice of Γ_n, as exemplified in Table 1?*

3. Isolated 2-PTMC's in Γ_2

In this section, we keep working in Γ_2, but slightly modifying the definition of a κ-PTMC by replacing the used Hamming distance h by the graph distance of Γ_2. It is clear that the Hamming distance in our graph-theoretical context is just the graph distance. Then, we have the following result.

Theorem 3.1. *There exists 262144 isolated 2-PTMC's in the 2-hive $[[\emptyset]] \subset \Gamma_2$.*

Proof. In Figure 4, the nine copies $\left[\begin{smallmatrix}xy\\ij\end{smallmatrix}\right]$, $(i, j \in F_3)$, of the tersquare are shown with its edges in thick black trace, against the thin black trace of the remaining edges of the 2-hive $[[\emptyset]]$. These nine copies happen to be the truncated 2-spheres centered at the vertices of an isolated PTMC of $[[\emptyset]]$ constituted as a selection of one vertex per yellow-faced 4-cycle in the figure. We may say that these yellow-faced 4-cycles are the "external" 4-cycles of $[[\emptyset]]$. So, there are $4^9 = 262144$ 2-PTMC's in Γ_2. □

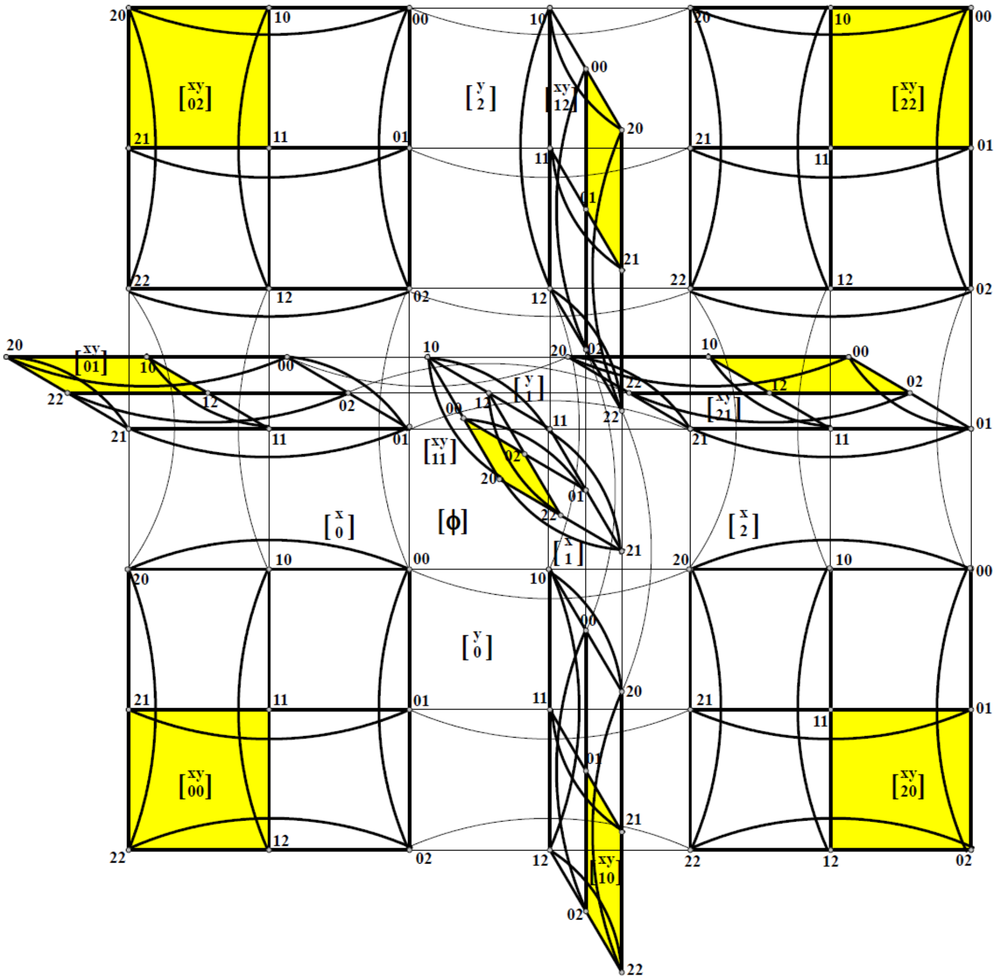

Fig. 4. Components of a 2-PTMC$[Q_2^2]$ of $[[\emptyset]]$ in Γ_2

Corollary 3.2. *There exists a 2-PTMC$[Q_2^2]$ in the 2-hive $[[\emptyset]]$.*

Proof. The yellow-faced 4-cycles are copies of Q_2^2 and induce the components of the claimed 2–PTMC-$[Q_2^2]$. □

Theorem 3.3. *There exists an infinite number of isolated 2-PTMC in Γ_2.*

Proof. Let us analyze one of the yellow squares in Figure 4, say square (00, 01,11,10) in tersquare $\left[\begin{smallmatrix} xy \\ 22 \end{smallmatrix}\right]$, as represented in Figure 5; the remaining eight yellow squares have similar properties to those to be described, once the notations of local vertices and neighboring tercubes are updated in each case in place of those in the figure. Besides the "external" 4-cycle $(00, 01, 11, 10)$ in Figure 5, whose edges are in black color, we set in red and blue, (green and hazel) colors those additional edges defining a pair of 4-cycles in the respective tercubes $\left[\begin{smallmatrix} xxy \\ 202 \end{smallmatrix}\right]$ and $\left[\begin{smallmatrix} xxy \\ 212 \end{smallmatrix}\right]$, ($\left[\begin{smallmatrix} xyy \\ 220 \end{smallmatrix}\right]$ and $\left[\begin{smallmatrix} xyy \\ 221 \end{smallmatrix}\right]$), namely $\{(00, 02, 12, 10), (01, 02, 12, 11)\}$, $(\{(00, 20, 21, 01), (10, 20, 21, 11)\})$, equally denoted but pertaining to different tersquares, as shown.

Since it is seen that the maximum truncated distance in Figure 5 is 2, we conclude that any one of the four vertices of the black 4-cycle dominates the remaining vertices in the other 4-cycles in the figure, in positions in their tersquares similar to those of the yellow cycles in Figure 4, namely the four just mentioned tersquares as well as the "opposite" tersquares $[\substack{xxyy\\2020}]$,$[\substack{xxyy\\2021}]$, $[\substack{xxyy\\2120}]$ and $[\substack{xxyy\\2121}]$, where these involved tersquare denominations are set in Figure 5 straddling edges common to two of their 4-cycles, for better reference, twice for the last four mentioned tersquares. This particular case is easily generalized to conclude that each vertex in a yellow square dominates via ρ in the neighboring tersquares in a form similar to that of $[[\emptyset]]$.

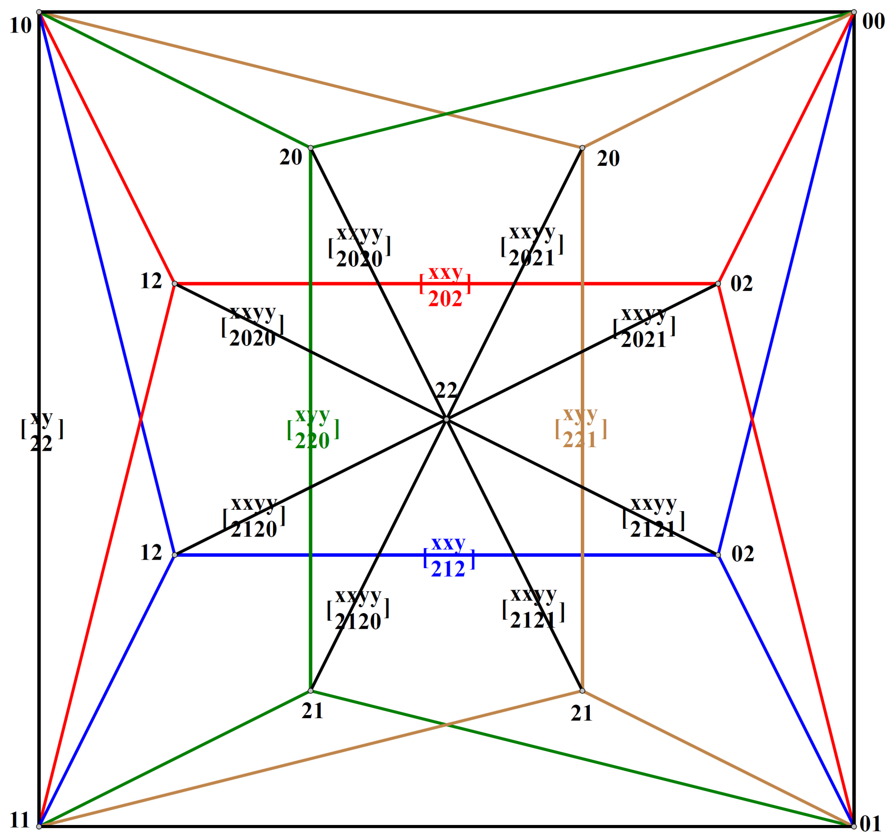

Fig. 5. Analysis of the square $(00, 01, 11, 10)$ in tersquare $[\substack{xy\\22}]$

With the same structure as the 2-hive $[[\emptyset]]$, we have the 2-hives of its neighboring 2-hive pair $\{[[\substack{xxx\\010}]], [[\substack{xxx\\012}]]\}$, etc., sharing four tersquares with $[[\emptyset]]$, tersquares denoted $(10, 11, 12)$, both in $[\substack{x\\0}]$ and in $[\substack{xy\\00}]$ and $[\substack{xy\\01}]$ and $[\substack{xy\\02}]$. These four tersquares belong both in $[[\substack{xxx\\010}]]$ and $[[\substack{xxx\\012}]]$ to the four respective tercubes $[\substack{xx\\01}]$, $[\substack{xxy\\010}]$, $[\substack{xxy\\011}]$ and $[\substack{xxy\\012}]$. Moreover, the union of these four tercubes constitutes the intersection $[[\substack{xxx\\010}]] \cap [[\substack{xxx\\012}]]$. By considering in each of these two 2-hives the equivalent of the yellow squares of $[[\emptyset]]$ in Figure 4, and selecting in each such yellow square a vertex contributing to the construction of an isolated 2-PTMC of Γ_2,, iteration of such a procedure eventually allows the completion of such dominating set. Observe that the argument exposed from the 2-hive pair $\{[[\substack{xxx\\010}]], [[\substack{xxx\\012}]]\}$ is one of twelve cases arising from the 2-hive $[[\emptyset]]$. Iteration of these twelve cases departing from any 2-hive of Γ_2 that is reached in the continuing procedure allows to advance a further step in the construction of such isolated 2-PTMC. □

Remark 3.4. The argument of Theorem 3.3 can be modified to ascertain the existence of 2-PTMC[H], where H is a 4-cycle, or the union of yellow squares with a common vertex in different 2-hives, like the eight squares, in Figure 5, at vertex 10 in the tersquares $[\substack{xy\\2,2}]$, $[\substack{xxy\\202}]$. $[\substack{xxy\\212}]$, $[\substack{xyy\\220}]$, $[\substack{xyy\\221}]$, $[\substack{xxyy\\2020}]$, $\substack{xxyy\\2021}]$ and $[\substack{xxyy\\2120}]$.

Conjecture 3.5. *There exists an isolated n-PTMC in Γ_n, $\forall n > 2$.*

Question 3.6. *Does there exist a suitable way of declaring a susbset $S \subset V(\Gamma_n)$ to be periodic, or periodic-like, that extends the notion of periodicity of Λ_n at the end of Remark 1.7 to one in Γ_n? so that a replacement of the notion of "quotient" or "toroidal" graphs of Λ_n can be found that way for Γ_n?*

References

[1] C. Araujo, I. Dejter, and P. Horak. A generalization of lee codes. *Designs, Codes and Cryptography*, 70:77–90 (13 pages), 2014. https://doi.org/10.1007/s10623-012-9666-6.

[2] S. Buzaglo and T. Etzion. Tilings by $(0.5, n)$-crosses and perfect codes. *SIAM Journal on Discrete Mathematics*, 27:1067–1081 (14 pages), 2013. https://doi.org/10.1137/110839916.

[3] R. Calderbank. Different aspects of coding theory: ams short course, san francisco, ca. *Proceedings of Symposia in Applied Mathematics*, 50, 1995. https://doi.org/10.1090/psapm/050.

[4] A. Campello, G. C. Jorge, J. E. Strapasson, and S. I. R. Costa. Perfect codes in the ℓ_p distance. *European Journal of Combinatorics*, 53:72–85, 2016. https://doi.org/10.1016/j.ejc.2015.11.002.

[5] G. Cohen, I. Honkala, S. Litsyn, and A. Lobstein. *Covering Codes*. Elsevier, New York, NY, 1997.

[6] I. Dejter and A. Delgado. Perfect dominating sets in rectangular grid graphs. *Journal of Combinatorial Mathematics and Combinatorial Computing*, 70:177–196, 2009.

[7] I. Dejter and P. Weichsel. Twisted perfect dominating subgraphs of hypercubes. *Congressus Numerantium*, 57:67–78, 1993.

[8] I. J. Dejter, L. R. Fuentes, and C. A. Araujo. There is but one pds in $\mathbb{Z}^3$ inducing just square components. *Bulletin of the Institute of Combinatorics and its Applications*, 82:30–41, 2018.

[9] T. Etzion. Tilings with generalized lee spheres. In J.-S. No, editor, *Mathematical Properties of Sequences and Other Combinatorial Structures*, pages 181–198. Springer 726, New York, NY, 2003. https://doi.org/10.1007/978-1-4615-0304-0_19.

[10] T. Etzion. Product constructions for perfect lee codes. *IEEE Transactions in Information Theory*, 57:7473–7481, 2011. https://doi.org/10.1109/TIT.2011.2161133.

[11] L. R. Fuentes, I. J. Dejter, and C. A. Araujo. Rainbow perfect domination in lattice graphs. *Electronic Journal Graph Theory and Applications*, 6(1):95–112, 2018. https://dx.doi.org/10.5614/ejgta.2018.6.1.7.

[12] S. Golomb and K. Welch. Perfect codes in the lee metric and the packing of polyominoes. *SIAM Journal on Applied Mathematics*, 18:302–307, 1970.

[13] P. Horak and B. F. AlBdaiwi. Diameter perfect lee codes. *IEEE Transactions in Information Theory*, 58:5490–5499, 2012. https://doi.org/10.1109/TIT.2012.2196257.

[14] P. Horak and O. Grosek. A new approach towards the golomb-welch conjecture. *European Journal of Combinatorics*, 38:12–22, 2014. https://doi.org/10.1016/j.ejc.2013.10.010.

[15] P. Horak and D. Kim. 50 years of the golomb-welch conjecture. *IEEE Transactions in Information Theory*, 60:3048–3061, 2018. https://doi.org/10.1109/TIT.2017.2786675.

[16] M. Livingstone and Q. F. Stout. Perfect dominating sets. *Congressus Numerantium*, 79:187–203, 1990.

[17] F. J. Macwilliams and N. A. J. Sloane. *The Theory of Error-Correcting Codes*. Elsevier, New York, NY, 1977.

[18] P. Östergård and W. Weakly. Constructing covering codes with given automorphism. *Designs, Codes and Cryptography*, 16:65–73, 1999. https://doi.org/10.1023/A:1008326409439.

[19] P. M. Weichsel. Dominating sets in n-cubes. *Journal of Graph Theory*, 18:479–488, 1994. https://doi.org/10.1002/jgt.3190180506.

4. Appendix

On the left of Figure 6, an oriented representation of a ternary square is provided. Here, one may take the vertices as decision conditional diamonds, the outgoing arrows as "Yes" or "True" option arrows and the incoming arrows as "No" or "False" option arrows. An elementary flowchart modeled on this oriented ternary square is given as an example on the right of Figure 6, where the root of the flowchart corresponds to vertex 00 and there are four terminators, corresponding to the vertices 01, 02, 11 and 12. The decision conditional diamonds correspond to the vertices 00, 10, 20, 21 and 22. To avoid terminators that are the end of more than one process, as is the case of 11 and 12 in the figure, one may select in Γ_2 modeling flowchart continuation in adjacent tercubes to the immediately previous ones, each sharing with the current tercube an already used triangle.

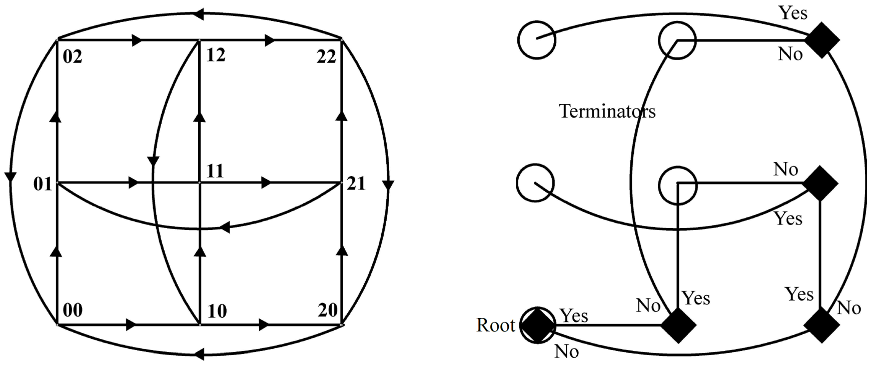

Fig. 6. Ternary square as a model of algorithm flowchart